



# Melting Heat Transfer Effects on MHD Chemically Thermally Radiative Micropolar Fluid Flow towards Stretching Exponentially Sheet with Heat Sink/Source

Shaik Mohammed Ibrahim<sup>1</sup>, Bommanna Lavanya<sup>2,\*</sup>, Gurram Dharmaiah<sup>3</sup>, Thummala Sankar Reddy<sup>4</sup>, Parakapali Roja<sup>5</sup>

<sup>1</sup> Department of Mathematics, Koneru Lakshmaiah Education Foundation, Green Fields, Vaddeswaram andhra Pradesh 522302, India

<sup>2</sup> Department of Mathematics, Manipal Institute of Technology, Manipal Academy of Higher Education, Manipal, Karnataka 576104, India

<sup>3</sup> Department of Mathematics, Narasaraopeta Engineering College, Narasaraopet Andhra Pradesh 522601, India

<sup>4</sup> Department of Mathematics, Annamacharya Institute of Technology and Sciences, C. K. Dinne Andhra Pradesh 516003, India

<sup>5</sup> Department of Mathematics, Annamacharya Institute of Technology and Sciences, Rajampeta Andhra Pradesh 516126, India

## ARTICLE INFO

### Article history:

Received 17 August 2024

Received in revised form 15 November 2024

Accepted 17 December 2024

Available online 31 January 2025

### Keywords:

Thermal radiation; melting heat transfer; MHD; micropolar; heat source/sink; chemical reaction

## ABSTRACT

The effective use of non-Newtonian fluids is vital for situations involving heat and mass transfer. For instance, we employ thermal paste, a non-Newtonian fluid, to cool the CPU. By means of a computational approach, the behaviour of non-Newtonian on the surface of a two-dimensional steady MHD boundary layer flow and melting heat and mass transfer over a micropolar fluid is presented here, in conjunction with a partially slipper sheet at the surface providing heat generation/absorption. Further, heat radiation as well as chemical reactions are considered. Using similarity parameters, the governing nonlinear partial differential equations for heat, mass and flow are converted into a series of coupled nonlinear ordinary differential equations, then solved using the Runge–Kutta fourth order integration scheme and the shooting method. For various parameters defining the flow within the boundary layer, the new findings for velocity, microrotation, temperature and concentration are graphed. Graphic representations of local skin friction, Nusselt number and Sherwood number are provided. Boosting the melting parameter decreases fluid velocity, microrotation and temperature significantly. An intensification in slip near the boundary decreases both fluid velocity and microrotation, but opposite effects are observed on temperature.

## 1. Introduction

The recent discovery of micro-polar fluids has attracted significant attention from engineering and scientific communities due to their unique characteristics compared to Newtonian fluids. Unlike Newtonian fluids, micro-polar fluids exhibit microrotation effects, allowing them to model more complex behaviours in certain applications, including biological and industrial processes. In addition to being non-Newtonian fluids, micropolar fluids exhibit microscopic effects, such as micro rotational

\* Corresponding author.

E-mail address: [lavanya.b@manipal.edu](mailto:lavanya.b@manipal.edu) (Bommanna Lavanya)

inertia. In view of its widespread application in manufacturing as well as in trade, micropolar fluids are a popular area of research. Navier-Stokes model has some limitations, notably lists, Fluids with efficient and effective applications cannot be described and explained by it. Sharma *et al.*, [1] in this paper discussed penetrable continuously stretched sheets along with slip impacts as a result of porous media cause thermal mass transfer in MHD micropolar fluids. An Analytical approach by Saraswathy *et al.*, [2] examines nonlinear radiative and dissipative, combine to cause MHD micropolar fluid to flow in porous channels. In this study, they examined the mixed cited impacts with the magnetic field on porous media. Microchannel thermal analysis by Narla *et al.*, [3] examined micropolar liquid flow ambitious with electroosmosis and peristalsis. The significance of micropolar liquids is taken into account when developing a model for heat transfer in thermally micropolar liquids on curved microchannels. Hydrodynamic behaviour analysis and the application of the micropolar fluids model utilizing user-defined functions in FLUENT studied by Wang *et al.*, [4]. In this paper they discussed FLUENT software was used to implement user-defined functions and analyse micropolar fluid behaviour and micropolar parameter values. A Poiseuille flow was used to compare user-defined function programs with the correctness of the solutions. An affecting particle, sliders bearing, dam breaks were used to analyse hydrodynamic behaviour in the Poiseuille flow. Many authors like Pasha *et al.*, [5], Karvelas *et al.*, [6], Vanitha *et al.*, [7], Srinivasacharya *et al.*, [8], Kocić *et al.*, [9] and Zhu *et al.*, [10] studied about micropolar fluids.

For the purpose of improving current energy devices and coming up with novel concepts, research on ways to increase heat transfer rate is essential. The key to optimizing cooling efficiency seems to be choosing a suitable working liquid coolant, aside from the sufficiency of the engineering procedure. Water, ethylene glycol and motor oil are examples of working fluids. Their main drawback is that these common fluids have far poorer thermal conductivities when compared to metals, metal oxides or carbon nanotubes, for example. Many new research areas with promising results have been inspired by the idea of suspending materials in the form of nanoparticles in standard base fluids to boost the thermal conductivity. Researchers and scientists are so focused on improving heating and cooling rates. Musa *et al.*, [11] studied analysing magneto-nanofluid through shrinking surfaces using nonlinear thermal radiation and melting heat transfer. Later Akinshilo *et al.*, [12] presented Microchannels embedded in vertical porous layers: the effect of melting and radiation. A porous microchannel within conductive and non-conducting surfaces is examined to determine whether slippery-melting affect mixed convection heat transmission. A detailed review about the melting heat and mass transfers can be found in Lee *et al.*, [13], Ramzan *et al.*, [14], Yang *et al.*, [15], Narender *et al.*, [16], Sushma *et al.*, [17], Anand Kumar *et al.*, [18], Kumar *et al.*, [19] and Ebiwareme *et al.*, [20].

The term magnetohydrodynamics (MHD) refers to the properties of a fluid's magnetic field in reaction to an electromagnetic force. Experts in fluid dynamics have recently become interested in MHD fluid flow along application to permeable media heat exchangers. These occurrences are receiving more attention because to their diverse functions in the scientific and industrial domains. There are many applications in areas of magneto patterns such as nuclear power plants, mining, plasma exploration, polymer exercising, geothermal extraction, production, refinement, radiative activation waste disposals and many others. Several insightful examinations been conducted on nanofluid flow in MHD absorbent medium. Sheikholeslami *et al.*, [21] proposed nanofluid flow in a porous channel with a transverse uniform magnetic regime using a Galerkin and least squares approach. A study by Reddy *et al.*, [22] focused on turbulent MHD nanofluid flow in permeable medium near a vertical plane. Bhatti *et al.*, [23] studied stretchable cylinder affected magneto nanofluid flow characteristics. Tistomo *et al.*, [24] studied thermal radiation effect measurement in enclosure calibration. Shah *et al.*, [25] reported a chemical reaction Carreau fluid with MHD boundary layer was discussed regarding radiation on convective heat transfer implications. A detailed study of

MHD in many fields studied by Harish *et al.*, [26], Magyari *et al.*, [27], Bidin *et al.*, [28], Ishak [29] and Khan *et al.*, [30].

Studying heat and mass transport in chemical reactions is necessary due to the increased requirement for chemical reactions in the chemical and hydrometallurgical sectors. Any type of chemical reaction occurs when a foreign substance is present in air or water. This could exist alone or in combination with water or air. The fluid through which the plate is flowing and an external mass react chemically in various chemical engineering operations. These procedures are used in many industrial applications, such as the processing of food, the creation of polymers and the production of ceramics or glassware. Recent studies have focused on coupled heat and mass transfer issues in chemical reactions because of their importance in numerous processes. Khan *et al.*, [31] studied heat-mass transfer on transient Riga plate stagnation point flow with chemical reaction and radiation. Study of chemical reactions between nanofluids and permeable stretching sheets with slip boundary layer flows studied by Vijaya *et al.*, [32]. Li *et al.*, [33] examined activation energy, Darcy–Forchheimer, chemical reaction on dissipative MHD squeezed flow on horizontal channels. In this study, activation energy and chemical reactions are investigated in relation to flow rate in a horizontal channel across which two parallel plates are moving using magnetohydrodynamic Darcy–Forchheimer squeezed Casson fluid flow. Chemical reaction and radiation impact on magneto flow of Oldroyd-B fluid through permeable medium by Salah *et al.*, [34]. Mahabaleshwar *et al.*, [35] conferred Navier's slip on hydromagnetic nano liquid flows and mass transfers. A detailed review of heat and mass transfer found in Singh *et al.*, [36], Roja *et al.*, [37], Mukhopadhyay [38], Mabood *et al.*, [39], Mandal *et al.*, [40] and Lavanya *et al.*, [41].

A goal of the application is to scrutinized the melting heat transfer over a micropolar fluid in two dimensions in a magneto steady flow across the boundary layer caused by stretchable expeditiously sheet with partial slip near the surface. Chemical reaction, radiation and heat sink/source are accounted. The consequences of the chemical reaction and thermal radiation are also considered. A set of coupled nonlinear ordinary differential equations is calculated using similarity variables for the nonlinear partial differential equations governing mass, flow and heat transfer. The Runge–Kutta fourth order integration scheme is then used to solve these equations numerically. For several parameters that describe the flow, the innovative results for the temperature, concentration, microrotation and dimensionless velocity within the boundary layer are shown visually. We investigated and visually displayed the Sherwood number, Nusselt number and local skin friction.

## 2. Methodology

The problem is modelled graphically in Figure 1, which includes the flow configuration and coordinate system, along with a detailed mathematical formulation. In this setup, a micropolar fluid flows steadily over an exponentially stretching sheet that is melting at a constant rate, creating a two-dimensional flow of an incompressible, electrically conducting fluid. The unique properties of the micropolar fluid, along with the exponential stretching and melting conditions, allow for an intricate flow dynamic influenced by the electrical conductivity and micropolar characteristics of the fluid.

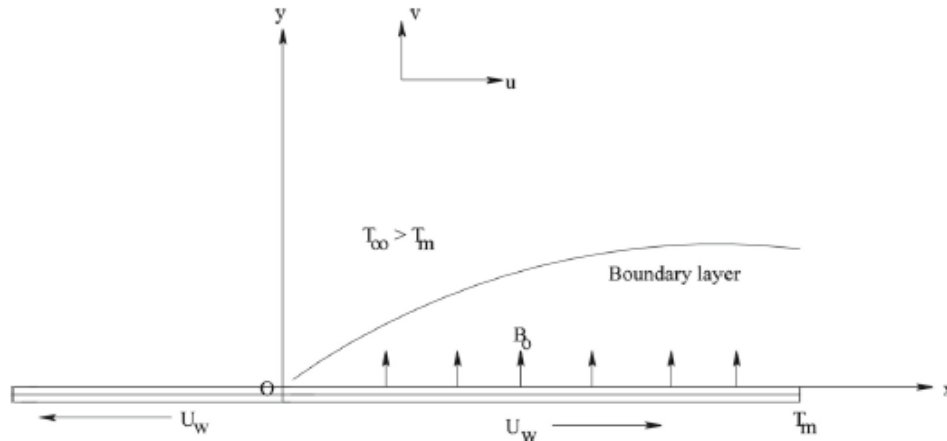


**Fig. 1.** Physical geometry of the fluid flow

A magnetic field of strength  $B = B_0 e^{\frac{x}{2L}}$ ,  $B_0$  is a constant is imposed in the normal direction of motion. Velocity  $U_w = ae^{\frac{x}{L}}$  where  $a (>0)$  is constant. A laminar flow dissipates less heat than viscous flow. Stress work effects are omitted here as well. Following are the governing equations that represent flow under these assumptions Mandal *et al.*, [40]:

Continuity:

$$u \frac{\partial u}{\partial x} + v \frac{\partial u}{\partial y} = 0, \quad (1)$$

Momentum:

$$u \frac{\partial u}{\partial x} + v \frac{\partial u}{\partial y} = u_e \frac{\partial u}{\partial x} + \left( \frac{\mu + K}{\rho} \right) \frac{\partial^2 u}{\partial y^2} + \frac{K}{\rho} \frac{\partial N}{\partial y} - \frac{\sigma B_0^2 u}{\rho} + g\beta_T(T - T_\infty) + g\beta_C(C - C_\infty), \quad (2)$$

Angular momentum:

$$u \frac{\partial N}{\partial x} + v \frac{\partial N}{\partial y} = \frac{\gamma}{\rho j} \frac{\partial^2 N}{\partial y^2} - \frac{K}{\rho j} \left( 2N + \frac{\partial u}{\partial y} \right), \quad (3)$$

Energy:

$$u \frac{\partial T}{\partial x} + v \frac{\partial T}{\partial y} = \frac{k}{\rho c_p} \frac{\partial^2 T}{\partial y^2} - \frac{1}{\rho c_p} \frac{\partial q_r}{\partial y} + \frac{Q_0}{\rho c_p} (T - T_\infty), \quad (4)$$

Concentration:

$$u \frac{\partial C}{\partial x} + v \frac{\partial C}{\partial y} = D \frac{\partial^2 C}{\partial y^2} - k(C - C_\infty). \quad (5)$$

$u, v$  refers the flow velocities,  $N$  refers microrotation,  $\mu, \rho, \nu = \frac{\mu}{\rho}$  refers fluid viscosity, density, kinematic viscosity,  $\sigma$  refers electrical conductivity,  $j, \gamma, K = \frac{\kappa}{\mu}$  refers microinertia, viscosity and material parameter,  $\kappa$  refers vortex viscosity,  $N$  refers microrotation,  $T, T_m, T_\infty$  refers fluid temperature, melting surface, free-stream,  $L$  refers length,  $k$  refers thermal conductivity,  $c_p$  refers specific heat,  $g$  refers acceleration,  $\beta$  refers thermal expansion volumetric coefficient,  $\beta_T$  and  $\beta_C$  refers thermal and volumetric expansion coefficients.  $C$  refers fluid concentration,  $Q$  refers heat sink/source coefficient, intended as  $Q = Q_0 \exp\left(\frac{x}{L}\right)$ ,  $Q_0$  refers heat sink/source constant coefficient, ( $Q_0 > 0$  &  $Q_0 < 0$  refers heat source/heat sink),  $\mu$  refers dynamic viscosity,  $D$  refers molecular diffusivity and  $k = k_0 \exp\left(\frac{x}{L}\right)$  refers first-order irreversible chemical reaction variable rate.

Spin gradient viscosity  $\gamma = \left(\mu + \frac{k}{2}\right)j = \mu\left(1 + \frac{K}{2}\right)j$ ,  $j = \frac{2Lve^{-\frac{x}{L}}}{a}$ . The boundary conditions for the model are as follows

$$u = u_w + u_{slip}, N = -n \frac{\partial u}{\partial y}, T = T_m, C = C_m \text{ at } y = 0, \quad (6)$$

$$u \rightarrow 0, N \rightarrow 0, T \rightarrow T_\infty, C \rightarrow C_\infty \text{ as } y \rightarrow \infty.$$

$$\text{and } k \left(\frac{\partial T}{\partial y}\right)_{y=0} = \rho [\lambda + c_s (T_m - T_0)] v(x, 0).$$

The slip velocity  $u_{slip} = \chi(x) \frac{\partial u}{\partial y}$ ,  $\chi(x) = Ae^{-\frac{x}{2L}}$ ,  $A, \lambda, c_s$  are constants, Rosseland estimate for emission is

$$q_r = -\frac{4\sigma^* \partial T^4}{3k^* \partial y}, \quad (7)$$

where  $\sigma^*, k^*$  are respectively, the Stefan–Boltzman constant and the mean absorption coefficient. We assume that the temperature differences within the flow are sufficiently small such that  $T^4$  may be expressed as a linear function of temperature. This is accomplished by expanding  $T^4$  in a Taylor's series about  $T_\infty$  and neglecting higher-order terms, thus

$$T^4 = T_\infty^4 + 4T_\infty^3(T - T_\infty) = 4T_\infty^3 T - 3T_\infty^4. \quad (8)$$

By using Eq. (7) and Eq. (8), Eq. (4) becomes

$$u \frac{\partial T}{\partial x} + v \frac{\partial T}{\partial y} = \frac{k}{\rho C_p} \frac{\partial^2 T}{\partial y^2} + \frac{16\sigma_1}{3\rho C_p k_1} \frac{\partial^2 T}{\partial y^2} + \frac{Q}{\rho C_p} (T - T_\infty). \quad (9)$$

Introducing the following dimensionless variables and quantities Mandal *et al.*, [40]:

$$\eta = y \sqrt{\frac{a}{2\nu L}} e^{\frac{x}{2L}}, u = a e^{\frac{x}{2L}} f'(\eta), v = -\sqrt{\frac{av}{2L}} e^{\frac{x}{2L}} [f(\eta) + \eta f'(\eta)], \quad (10)$$

$$\psi = \sqrt{2Lv} a e^{\frac{x}{2L}} f(\eta), N = \frac{a}{2\nu L} \sqrt{2Lv} a e^{\frac{3x}{2L}} g(\eta),$$

$$\theta(\eta) = \frac{T-T_\infty}{T_m-T_\infty}, \phi(\eta) = \frac{C-C_\infty}{C_w-C_\infty}.$$

Now, the Eq. (2), Eq. (3), Eq. (5) and Eq. (9) simplify into the nonlinear self-similar ordinary differential equations described below:

$$(1 + K)f''' + ff'' - f'^2 - Mf' + Kg' = 0, \quad (11)$$

$$(1 + K/2)g'' + fg' - f'g - K(2g + f'') = 0, \quad (12)$$

$$\left(1 + \frac{4}{3}R\right)\theta'' + Pr(f\theta' - f'\theta + 2\delta\theta) = 0, \quad (13)$$

$$\phi'' + Sc(f\phi' - f'\phi) - ScKr\phi = 0. \quad (14)$$

The transformed boundary conditions are

$$f'(0) = 1 + \chi f''(0), g(0) = -nf''(0), Pr f(0) + \alpha\theta'(0) = 0, \theta(0) = 1, \phi(0) = 1, \\ f'(\infty) = 0, g(\infty) = 0, \theta(\infty) = 0, \phi(\infty) = 0. \quad (15)$$

where primes denote differentiation with respect to  $\eta$  and

$$M = \frac{2L\sigma B_0^2}{\rho U_0}, Pr = \frac{\nu}{\alpha} = \frac{\rho\nu c_p}{k} = \frac{\mu c_p}{k}, \delta = \frac{Q_0 L}{a\rho c_p}, \\ R = \frac{4\sigma^* T_\infty^3}{k^* k}, Sc = \frac{\nu}{D}, Kr = \frac{K_0 L}{U_0}, \alpha = \frac{kc_p(T_\infty - T_m)}{\rho(\lambda + c_s(T_m - T_0))}. \quad (16)$$

$M, Pr, R, \delta, Kr, \alpha$  refers magnetic number, Prandtl number, thermal radiation parameter, heat absorption/generation parameter, chemical reaction parameter and melting parameter respectively

Skin friction coefficient  $C_f$ , Couple stress coefficient  $C_s$ , Nusselt number  $Nu$  and Sherwood number  $Sh$ , presented as:

$$C_f = \frac{\tau_w}{\rho u_w^2}, C_s = \left[(\mu + K/2)j \frac{\partial N}{\partial y}\right]_{y=0}, Nu = \frac{xq_w}{k(T_\infty - T_m)}, Sh = \frac{xq_m}{D(C_\infty - C_0)}. \quad (17)$$

Skin friction, surface heat and mass fluxes ( $\tau_w, q_m$  and  $q_n$ ) are:

$$\tau_w = \left[(\mu + k) \left(\frac{\partial u}{\partial y}\right)\right]_{y=0} + K(N)_{y=0}, q_m = -k \left(\frac{\partial T}{\partial y}\right)_{y=0} \text{ and } q_n = -D \left(\frac{\partial C}{\partial y}\right)_{y=0}. \quad (18)$$

Substituting Eq. (18) into Eq. (17) we obtained,

$$Cf_x = Re_x^{1/2} C_f = [1 + (1-n)K] f''(0), \tag{19}$$

$$Nu_x = Re_x^{1/2} Nu = -\theta'(0), \tag{20}$$

$$Sh_x = Re_x^{1/2} Sh = -\phi(0), \tag{21}$$

where  $Cf_x, Nu_x, Sh_x, Re_x = u_e(x)x/\nu$  are local skin friction, Nusselt number, Sherwood number, Reynolds numbers respectively.

### 3. Numerical Process

In order to resolve transformed Eq. (11) to Eq. (14) with boundary conditions Eq. (15) as an initial value problem:

- i. The initial guess values of  $f''(0), g'(0), \theta'(0)$  and  $\phi'(0)$  are chosen.
- ii. Next, Runge–Kutta–Fehlberg method is applied to obtain a solution.
- iii. The  $f'(\eta), g(\eta), \theta(\eta)$  and  $\phi(\eta)$  determined values at  $\eta = \eta_\infty$  ( $\eta_\infty$  refers sufficient large value of  $\eta$ ), compared with boundary conditions  $f'(\eta_\infty)=1, g(\eta_\infty)=0, \theta(\eta_\infty)=1$  and  $\phi(\eta_\infty)=1$ .
- iv. For  $f''(0), g'(0), \theta'(0)$  and  $\phi'(0)$  missing values, the shooting method is utilized.
- v. We have fixed  $K, M, \delta, R, Pr$  and  $n$ .
- vi. With the help of MATHEMATICA 11.0 software for various  $\Delta\eta$  size values, velocity, temperature, skin friction coefficient and local Nusselt number changed negligibly for value of  $\Delta\eta > 0.01$ . Consequently, step-size  $\Delta\eta = 0.001$  has been determined by the authors.
- vii. Methodology of the problem interpreted through flow chart in Figure 2.

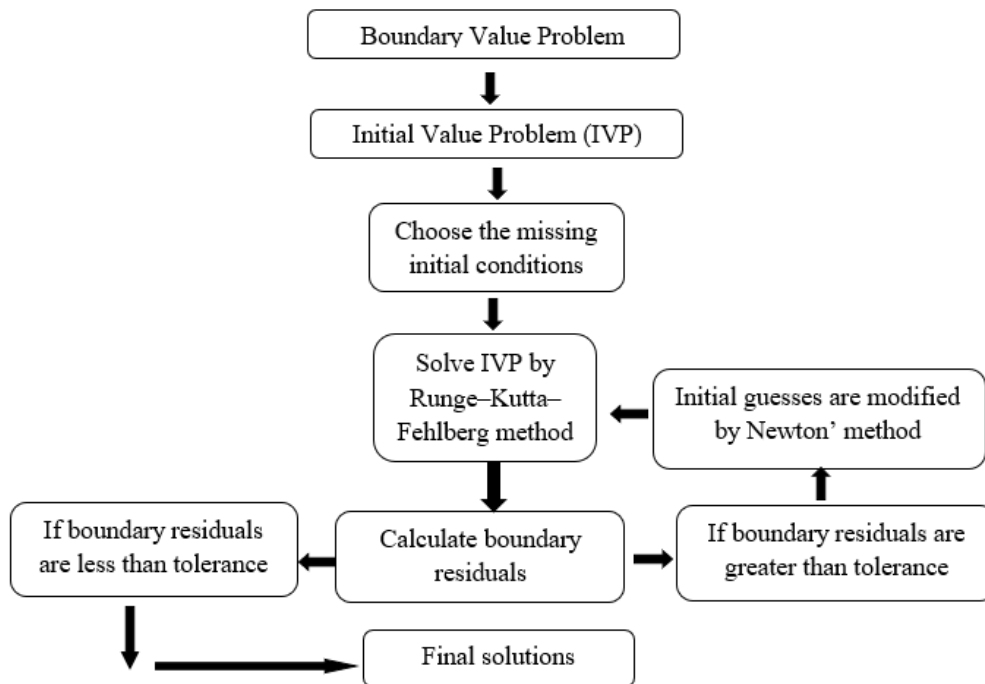


Fig. 2. Flow chart

### 4. Results and Discussion

To validate the solution of Eq. (11) to Eq. (14) Table 1 is presented.

**Table 1**

Comparison for the values of  $(-\theta'(0))$  corresponding to the ordinary viscous fluid ( $K = 0$ ) for some specific values of the governing parameters in nonappearance of thermal radiation, heat source/sink, chemical reaction and slip at the boundary

Magnetic Parameter (M)	Pandtl number (Pr)	Magyari <i>et al.</i> , [27]	Bidin <i>et al.</i> , [28]	Ishak [29]	Mukhopadhyay [38]	Mabood <i>et al.</i> , [39]	Mandal <i>et al.</i> , [40]	Present
0	1	0.954782	0.9548	0.9548	0.9547	0.95478	0.95475	0.954749
	2		1.4714	1.4715	1.4714	1.47148	1.47148	1.471478
	3	1.869075	1.8691	1.8691	1.8691	1.86907	1.86907	1.869069
	5	2.500135		2.5001	2.5001	2.50011	2.50011	2.500100
	10	3.6604		3.6604	3.6603	3.66039	3.66036	3.660358
1	1			0.8611	0.8610	0.86113	0.86105	0.861001

The influence of the parameters in the equations of the problem is evaluated using Figure 3(a) to 3(b) through Figure 15(a) to 15(b). This evaluation reveals the performance of the velocity, angular velocity, temperature and concentration fields, providing a clearer physical understanding of the problem.

Figure 3(a) and 3(b) illustrate the effects of microrotation and velocity under varying values of M and the melting heat parameter  $\alpha$ . As the value of M increases, the fluid velocity decreases. The Lorentz force, which is generated when magnetic fields are applied to flow fields, contributes to this decrease by impeding the motion of the fluid. This force slows down the fluid flow, leading to reduced velocity as the thickness of the momentum layer increases (see Figure 3(a)). Additionally, an increase in the value of M results in greater angular velocity near the sheet (refer to Figure 3(b)).

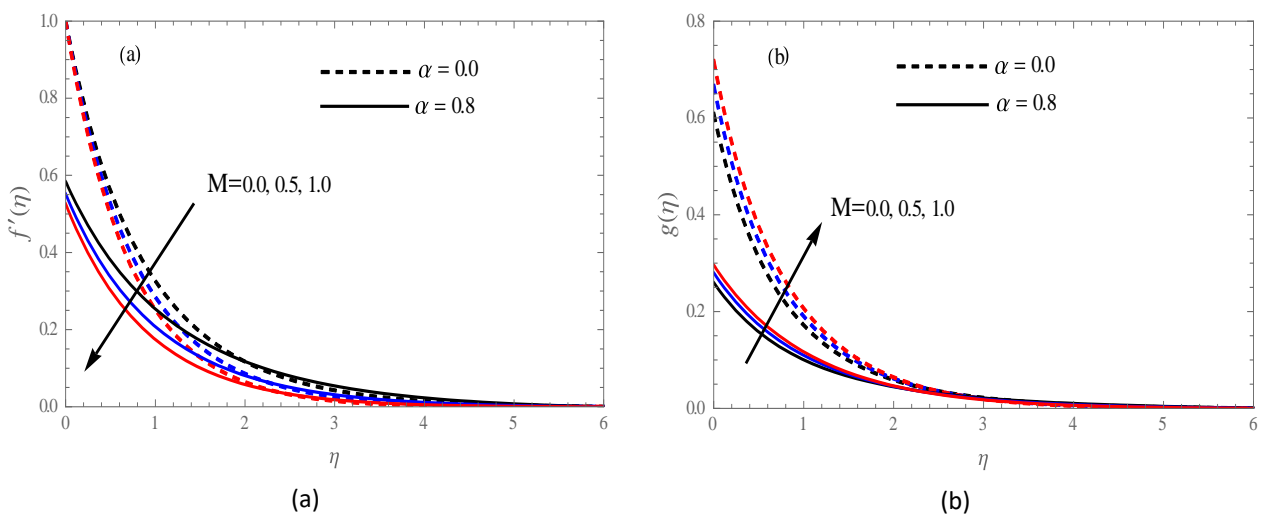
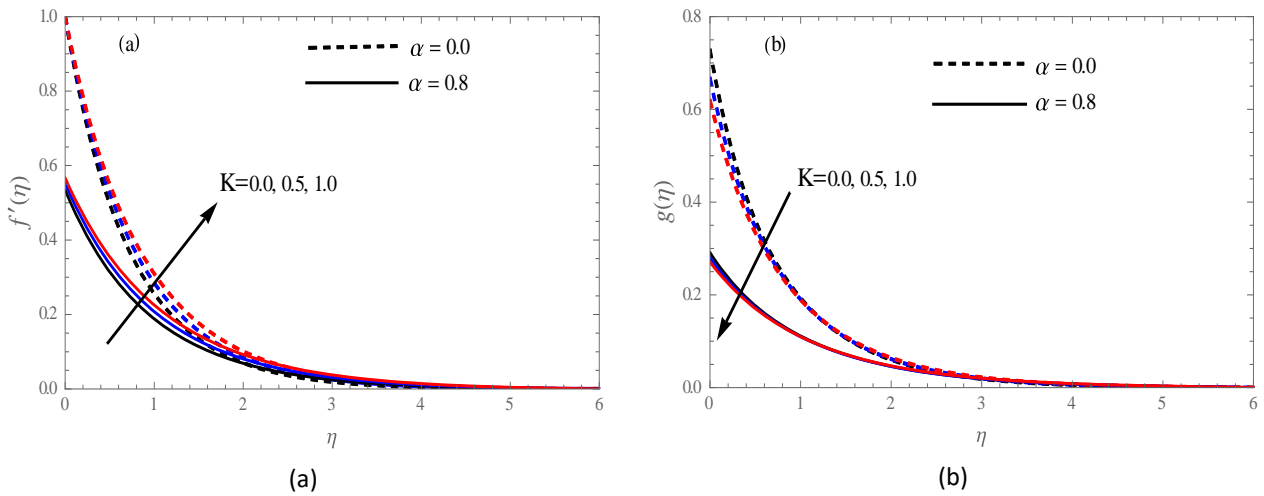


**Fig. 3.** (a) Velocity profiles for various M values (b) Microrotation profiles for various M values

As shown in Figure 4(a) and 4(b), for different values of K, there are differences in velocity and angular velocity. Microrotation diminishes as 'K' grows shown in Figure 4(a) while fluid velocity increases in Figure 4(b). It is the micropolar fluidity parameter (K) that determines the velocity profile

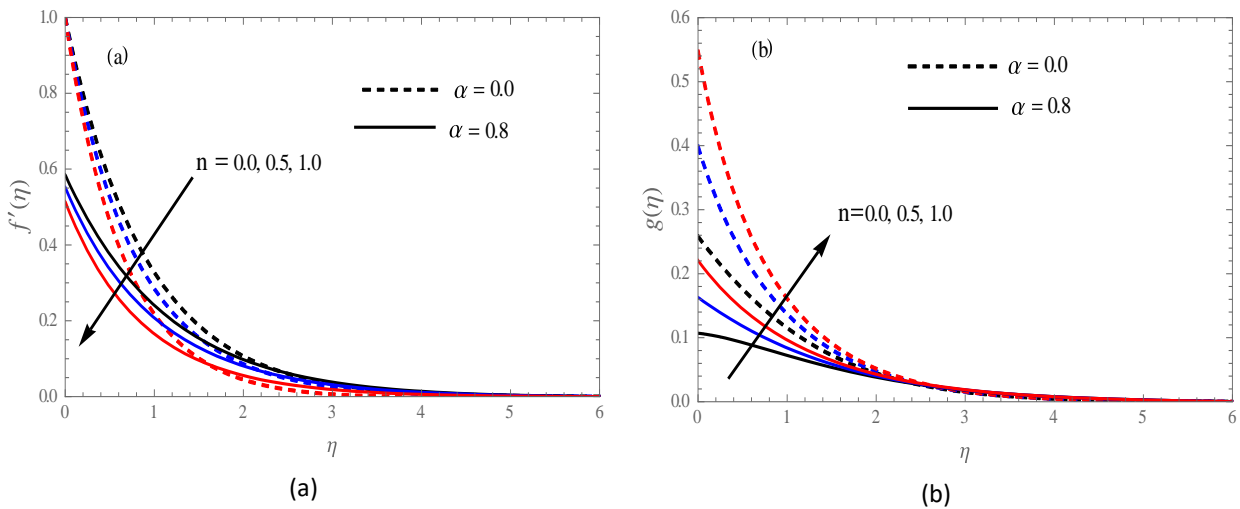


of micropolar fluids physically. The increase in the micropolarity parameter ( $K$ ) indicates a stronger influence of the microstructure on fluid flow.



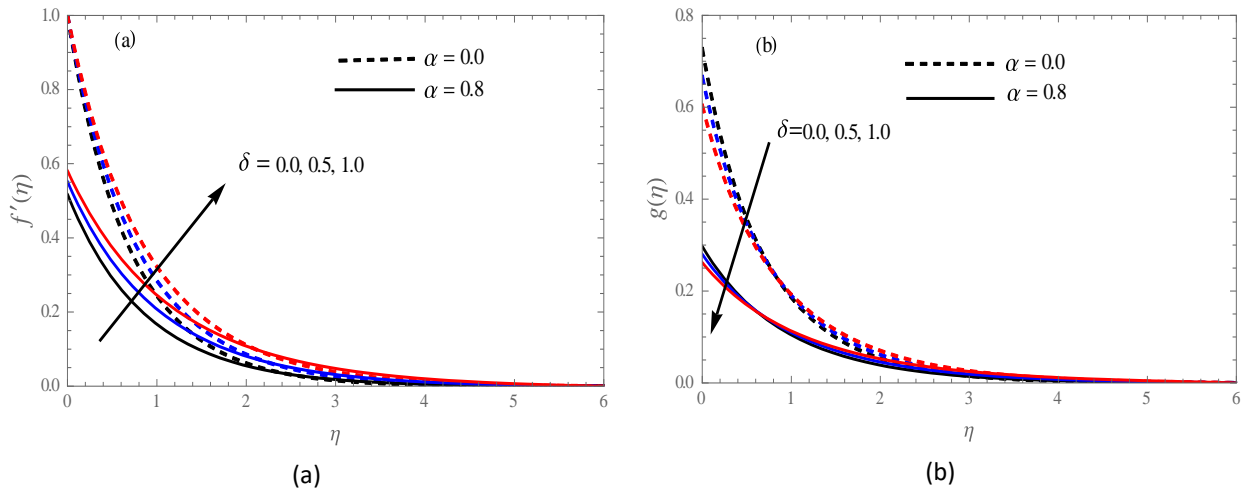
**Fig. 4.** (a) Velocity profiles for various  $K$  values (b) Microrotation profiles for various  $K$  values

As shown in Figure 5(a) and 5(b),  $n$  belongs to distributions of velocity and angular velocity. Figure 5(a) shows that velocity decreases with increasing  $n$ . It is found that microrotation increases with the acceleration value of  $n$  in Figure 5(b) up to a certain point.



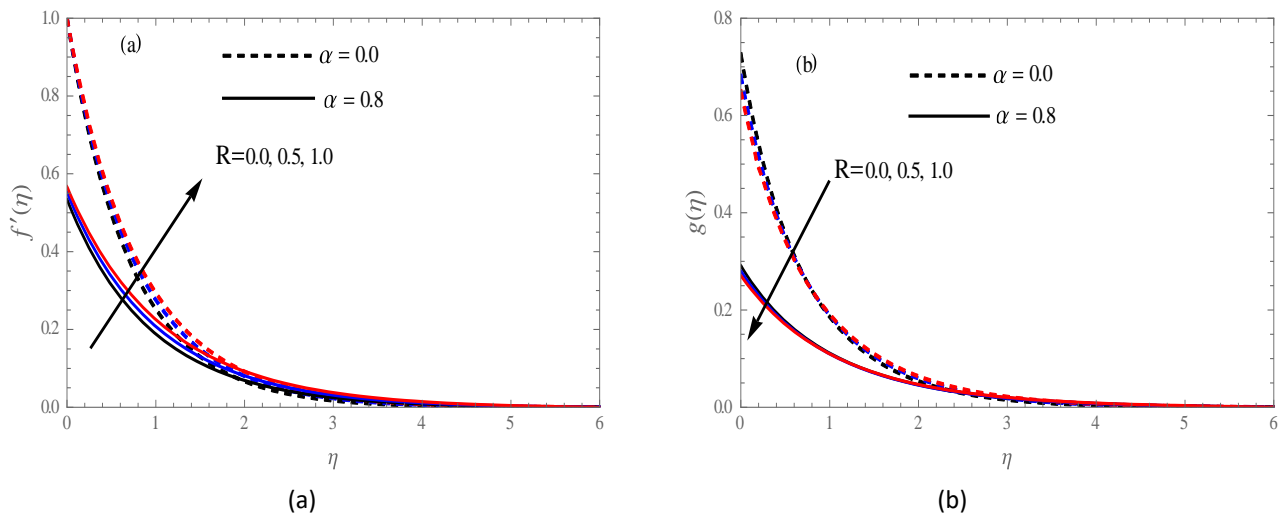
**Fig. 5.** (a) Velocity profiles for various  $n$  values (b) Microrotation profiles for various  $n$  values

In Figures 6(a) and 6(b) we observe that increase in heat source parameter records the increase in velocity in Figure 6(a) and as rising values of  $\delta$  we can observe the fall in angular velocity in Figure 6(b). An enhancing in velocity close to the surface occurs due to relative motion between fluid molecules along the surface. Moving from the surface to the bulk of the fluid causes the profile to increase.



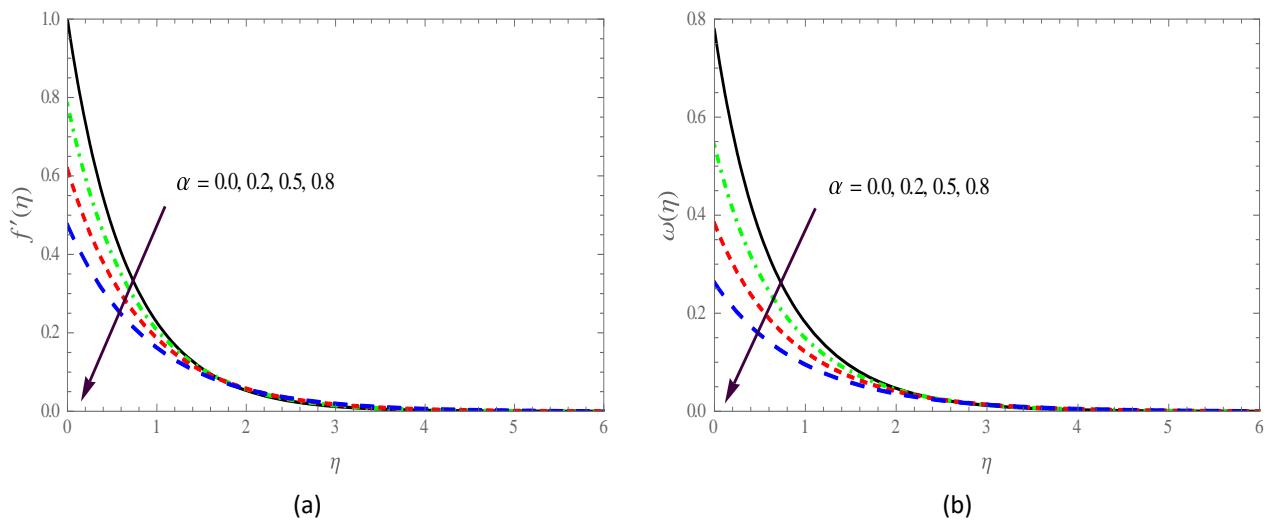
**Fig. 6.** (a) Velocity profiles for various of  $\delta$  values (b) Microrotation profiles for various  $\delta$  values

Figure 7(a) and 7(b) depict that as we increase the values of  $R$  we can observe velocity rises and microrotation decreases.



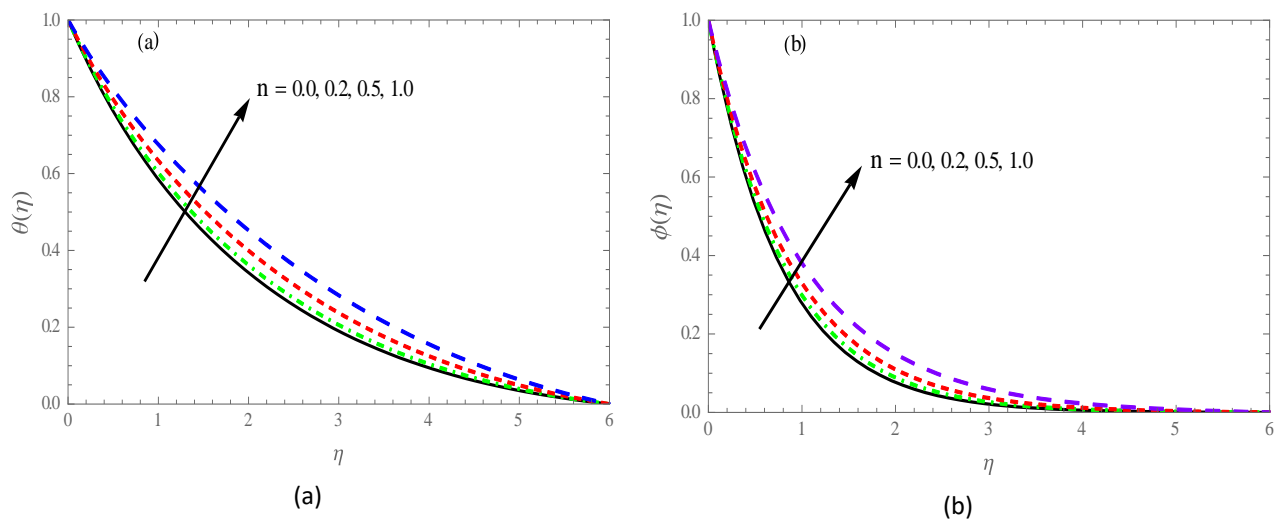
**Fig. 7.** (a) Velocity profiles for various  $R$  values (b) Microrotation profiles for various  $R$  values

As we rise in the values  $\alpha$  both velocity and angular velocity collapses that we presented in Figure 8(a) and 8(b). When the melting parameter  $\alpha$  increases, the melting parameter  $\alpha$  velocity increases as well. Detecting melting parameter  $\alpha$  in the presence of the stretched surface partially transmits the drawing into the fluid and thus reduces fluid velocity.



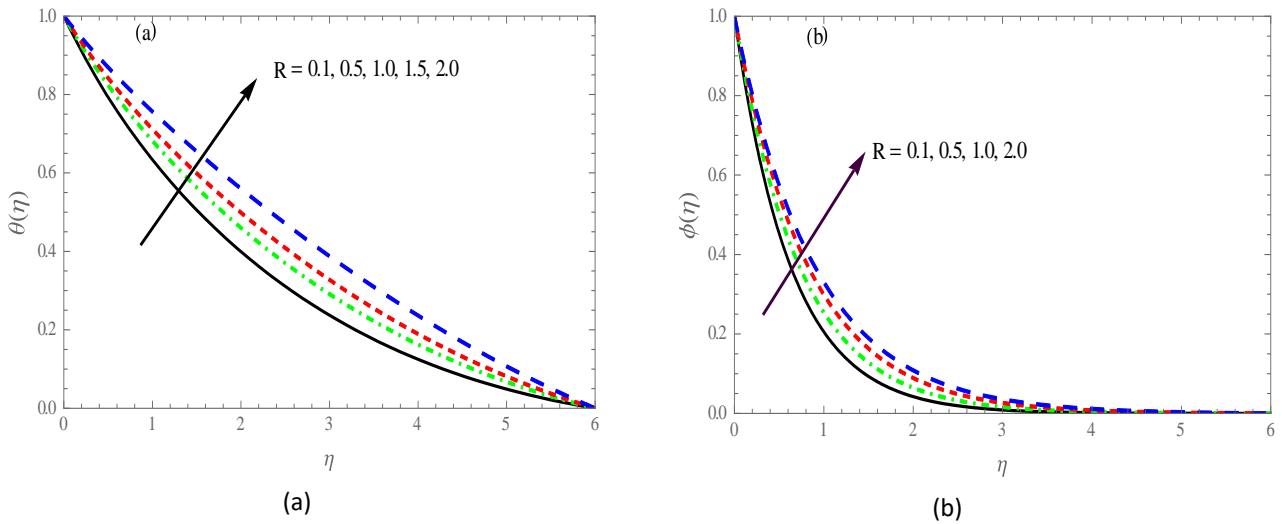
**Fig. 8.** (a) Velocity profiles for various  $\alpha$  values (b) Microrotation profiles for various  $\alpha$  values

Figure 9(a) and 9(b) portray the belongings of  $n$  on temperature and concentration sketches. An increase in the value of  $n$  depicts the rise in both temperature and concentration sketches, is noticed. It shows the growth in thermal boundary layer.



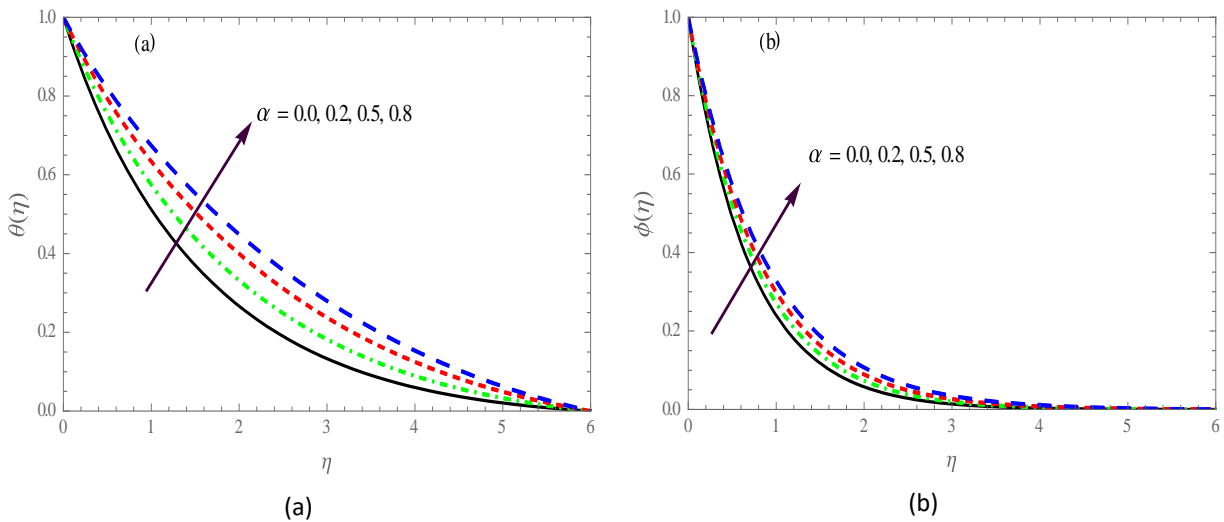
**Fig. 9.** (a) Temperature profiles for various  $n$  values (b) Concentration profiles for various  $n$  values

In Figure 10(a), a selection of values of  $R$  is shown to indicate a disparity of hotness. An increase in the values of  $R$  shows the growth in temperature profile, is noted. Melting parameters connected to micropolar fluids positively affect the fluid velocity, temperature and rotational speed of the fluids. Figure 10(b) represents the growth in concentration profiles by increasing  $R$  values.



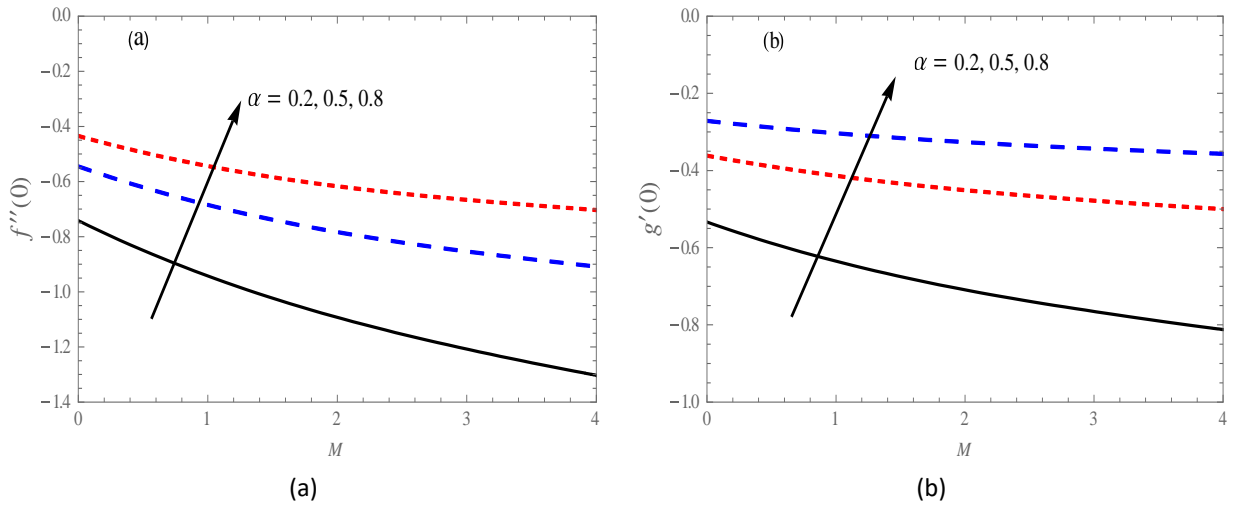
**Fig. 10.** (a) Temperature profiles for various  $R$  values (b) Concentration profiles for various  $R$  values

The growth in temperature and concentration with velocity slip parameter sketches is shown in Figure 11(a) and 11(b).



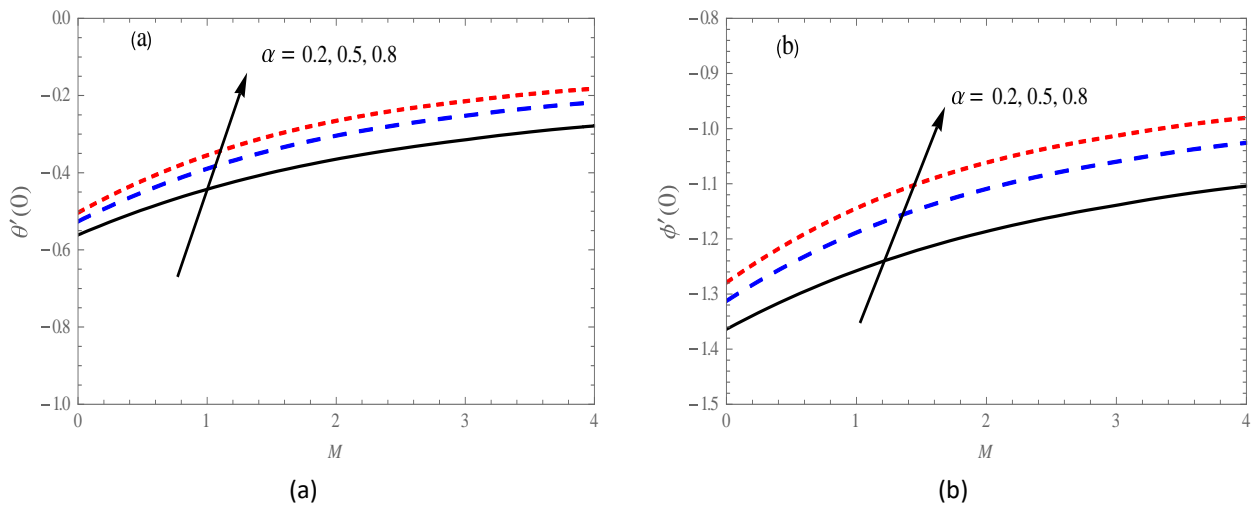
**Fig. 11.** (a) Temperature profiles for various  $\alpha$  values (b) Concentration profiles for various  $\alpha$  values

A plot of the variation of skin friction with magnetic field parameter  $M$  and melting parameter  $\alpha$  is shown in Figure 12(a). It is observed that as melting parameter  $\alpha$  is decreased, this decreases with an increase in  $\alpha$ . Compressibility, surface roughness and skin friction effects are discussed as are equivalent flat plate methods to calculate component drag in laminar and turbulent flow. Figure 12(b) displays the variation of wall couple stress with Magnetic field parameter  $M$  for dissimilar melting factor values  $\alpha$ . A frictional drag force opposes the motion of the body through the fluid due to the frictional shear stresses on its surface.



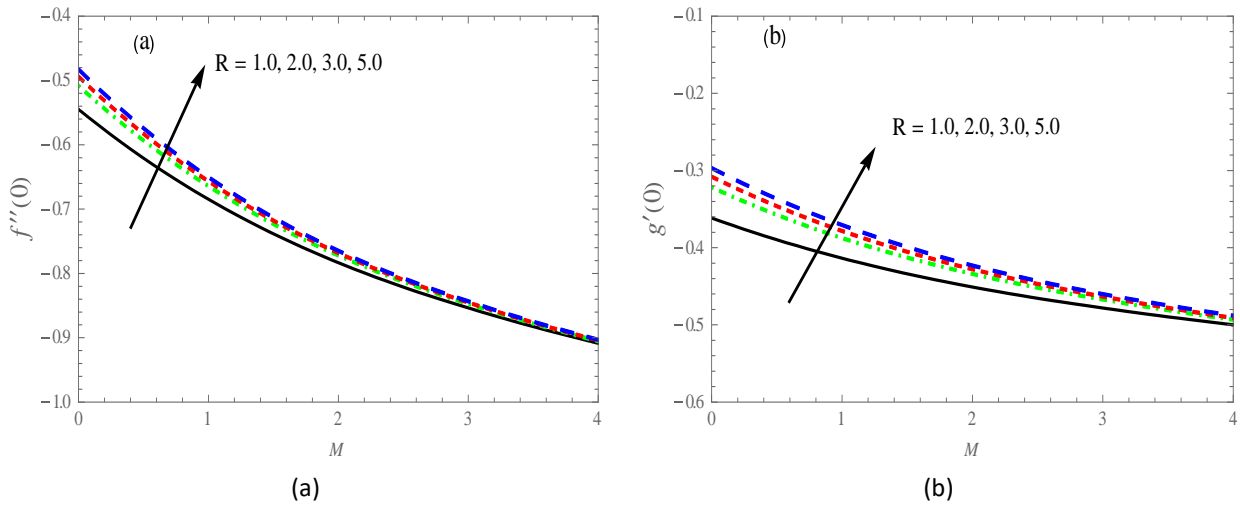
**Fig. 12.** (a) Skin friction coefficient for various  $M$  values (b) Couple stress coefficient for various of  $M$  values

Figure 13(a) shows the variation of temperature gradient at the wall with changing magnetic field parameter  $M$  for varying melting parameter  $\alpha$ . From this figure it is observed that Nusselt number increases as magnetic field and melting parameter  $\alpha$  increases. Figure 13(b) shows the variation in Sherwood number for different values of magnetic field parameter and melting parameter  $\alpha$ . It is noticed that an increasing values of  $M$  and  $\alpha$ , the concentration gradient is also increase.



**Fig. 13.** (a) Nusselt number for various of  $M$  values (b) Sherwood number for various of  $M$  values

Skin friction factor and rate of couple stress reduced with increasing of magnetic field parameter, but reverse behaviour observed for radiation parameter in Figure 14(a) and 14(b).



**Fig. 14.** (a) Skin friction coefficient for various of  $M$  values (b) Couple stress coefficient for various  $M$  values

With increasing values of  $R$  and  $M$ , the temperature gradient at the wall increases (Figure 15(a)). The concentration gradient close to the wall tends to increase as magnetic field parameter and radiation parameter increases, it is noted in Figure 15(b).

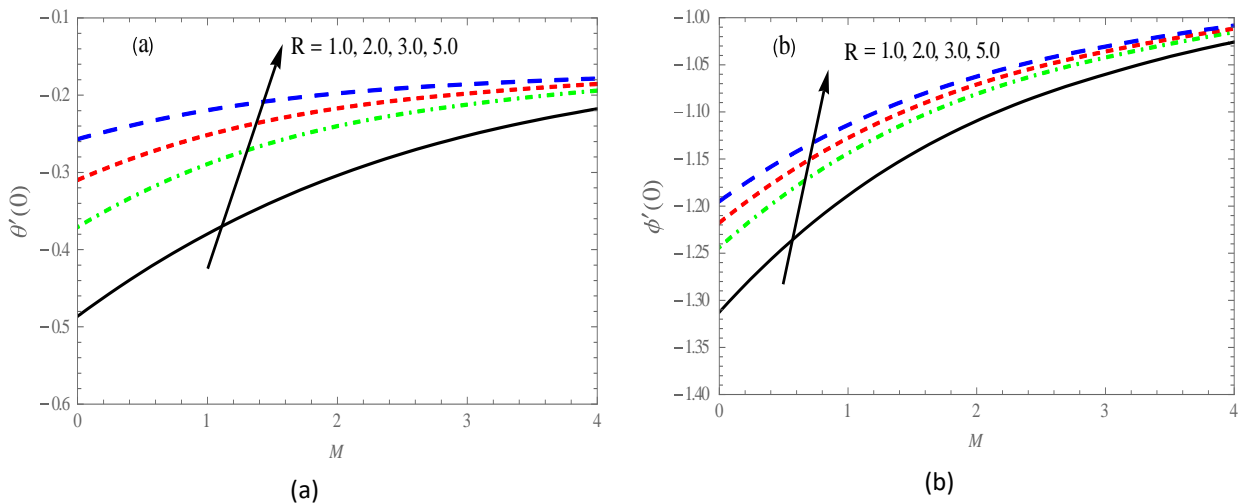


**Fig. 15.** (a) Nusselt number for various  $M$  values (b) Sherwood number for various  $M$  values

## 5. Conclusions

We have numerically analysed the combined effects of mass and melting energy transfer on the flow of an MHD micropolar fluid through a permeable porous medium. The impacts of thermal radiation, heat sink/source and chemical reactions have also been investigated under slip flow conditions. The main findings are as follows:

- i. Increasing the melting parameter leads to a decrease in fluid velocity, angular velocity and temperature.
- ii. Both fluid velocity and angular velocity diminish with higher slip at the boundary, while the temperature exhibits an opposite trend.

- iii. An increase in the material parameter results in higher fluid velocity but lower angular velocity.
- iv. Enhancing the magnetic factor causes a reduction in both velocity and angular velocity, while temperature increases.
- v. Velocity is inversely proportional to both the magnetic factor and slip parameter. Microrotation (angular velocity) decreases with the slip parameter and temperature rises with increasing magnetic factor and thermal radiation but decreases with a higher Prandtl number.
- vi. The surface shear stress increases with greater magnetic factor and slip parameter values.

## Acknowledgement

This research was not funded by any grant.

## References

- [1] Sharma, Surbhi, Amit Dadheech, Amit Parmar, Jyoti Arora, Qasem Al-Mdallal and S. Saranya. "MHD micro polar fluid flow over a stretching surface with melting and slip effect." *Scientific reports* 13, no. 1 (2023): 10715. <https://doi.org/10.1038/s41598-023-36988-3>
- [2] Saraswathy, M., D. Prakash and Putta Durgaprasad. "MHD micropolar fluid in a porous channel provoked by viscous dissipation and non-linear thermal radiation: an analytical approach." *Mathematics* 11, no. 1 (2022): 183. <https://doi.org/10.3390/math11010183>
- [3] Narla, V. K., Dharmendra Tripathi and D. S. Bhandari. "Thermal analysis of micropolar fluid flow driven by electroosmosis and peristalsis in microchannels." *International Journal of Ambient Energy* 43, no. 1 (2022): 8193-8205. <https://doi.org/10.1080/01430750.2022.2091034>
- [4] Wang, Lian, Xihua Chu, Ji Wan and Chenxi Xiu. "Implementation of micropolar fluids model and hydrodynamic behavior analysis using user-defined function in FLUENT." *Advances in Mechanical Engineering* 12, no. 7 (2020): 1687814020943052. <https://doi.org/10.1177/1687814020943052>
- [5] Pasha, Pooya, Saeid Mirzaei and Meysam Zarinfar. "Application of numerical methods in micropolar fluid flow and heat transfer in permeable plates." *Alexandria Engineering Journal* 61, no. 4 (2022): 2663-2672. <https://doi.org/10.1016/j.aej.2021.08.040>
- [6] Karvelas, Evangelos, Giorgos Sofiadis, Thanasis Papathanasiou and Ioannis Sarris. "Effect of micropolar fluid properties on the blood flow in a human carotid model." *Fluids* 5, no. 3 (2020): 125. <https://doi.org/10.3390/fluids5030125>
- [7] Vanitha, G. P., U. S. Mahabaleshwar, M. Hatami and Xiaohu Yang. "Heat and mass transfer of micropolar liquid flow due to porous stretching/shrinking surface with ternary nanoparticles." *Scientific Reports* 13, no. 1 (2023): 3011. <https://doi.org/10.1038/s41598-023-29469-0>
- [8] Srinivasacharya, D. and K. Hima Bindu. "Entropy generation of micropolar fluid flow in an inclined porous pipe with convective boundary conditions." *Sādhanā* 42 (2017): 729-740. <https://doi.org/10.1007/s12046-017-0639-3>
- [9] Kocić, Miloš, Živojin Stamenković, Jelena Petrović and Jasmina Bogdanović-Jovanović. "MHD micropolar fluid flow in porous media." *Advances in Mechanical Engineering* 15, no. 6 (2023): 16878132231178436. <https://doi.org/10.1177/16878132231178436>
- [10] Zhu, Weiyao. "Theoretical study of micropolar fluid flow in porous media." *Advances in Geo-Energy Research* 5, no. 4 (2021): 465-472. <https://doi.org/10.46690/ager.2021.04.11>
- [11] Musa, Awad, Aamir Hamid, Muhammad Yasir and Muzamil Hussain. "Effect of nonlinear thermal radiation and melting heat transfer assessment on magneto-nanofluid through a shrinking surface." *Waves in Random and Complex Media* (2022): 1-18. <https://doi.org/10.1080/17455030.2022.2084575>
- [12] Akinshilo, A. T., A. O. Ilegbusi, H. M. Ali, M. Sanusi and M. G. Sobamowo. "Impact of melting and radiation on MHD mixed convective heat transfer slip flow through vertical porous embedded micro-channel." *Journal of Central South University* 30, no. 11 (2023): 3670-3681. <https://doi.org/10.1007/s11771-023-5400-y>
- [13] Lee, Yee-Ting, Liang-Han Chien, Fan-Bill Cheung and An-Shik Yang. "Numerical and experimental investigations on melting heat transfer performance of PCM in finned cold thermal energy storage." *International Journal of Heat and Mass Transfer* 210 (2023): 124199. <https://doi.org/10.1016/j.ijheatmasstransfer.2023.124199>
- [14] Ramzan, Muhammad and Naila Shaheen. "Impact of melting heat transfer and variable characteristics on an MHD non-Newtonian shear-thinning fluid flow with gyrotactic microorganisms over a nonlinear stretched

- surface." *Journal of Applied Mathematics and Physics* 11, no. 8 (2023): 2461-2471. <https://doi.org/10.4236/jamp.2023.118157>
- [15] Yang, Hong, Aaqib Majeed, Kamel Al-Khaled, Tasawar Abbas, Muhammad Naeem, Sami Ullah Khan and Munazza Saeed. "Significance of melting heat transfer and Brownian motion on flow of Powell–Eyring fluid conveying nano-sized particles with improved energy systems." *Lubricants* 11, no. 1 (2023): 32. <https://doi.org/10.3390/lubricants11010032>
- [16] Narender, P. and T. Ramakrishna Goud. "Melting Heat Transfer on Magnetohydrodynamics-Nanofluid Boundary Layer Flow Past a Stretching Sheet: Thermal Radiation and Viscous Dissipation Effects." *Journal of Nanofluids* 12, no. 6 (2023): 1566-1576. <https://doi.org/10.1166/jon.2023.2040>
- [17] Sushma, T. C., N. Nalinakshi, P. A. Dinesh, D. V. Jayalakshamma and T. Sravan Kumar. "Convective heat transfer and MHD flow through semi-porous cylindrical filters embedded in an impermeable region." *Chinese Journal of Physics* 81 (2023): 9-25. <https://doi.org/10.1016/j.cjph.2022.10.015>
- [18] Anand Kumar, S. Abhilash, S. Sreedhar and M. Veera Krishna. "Heat and mass transfer on unsteady MHD convective flow through porous medium between two vertical plates with chemical reaction." *Proceedings of the Institution of Mechanical Engineers, Part E: Journal of Process Mechanical Engineering* 238, no. 4 (2024): 1665-1675. <https://doi.org/10.1177/09544089231160877>
- [19] Kumar, Vasa Vijaya, Mamidi Narsimha Raja Shekar and Shankar Goud Bejawada. "Heat and Mass Transfer Significance on MHD Flow over a Vertical Porous Plate in the Presence of Chemical Reaction and Heat Generation." *CFD Letters* 16, no. 5 (2024): 9-20. <https://doi.org/10.37934/cfdl.16.5.920>
- [20] Ebiwareme, Liberty and Kubugha Wilcox Bunonyo. "MHD Fluid Flowing through a Vertical Porous Plate with the Influence of a Magnetic Field and an Angle of Inclination Using the Method of Reduced Differential Transformation." *Asian Journal of Pure and Applied Mathematics* (2023): 179-193.
- [21] Sheikholeslami, M., M. Hatami and D. D. Ganji. "Analytical investigation of MHD nanofluid flow in a semi-porous channel." *Powder Technology* 246 (2013): 327-336. <https://doi.org/10.1016/j.powtec.2013.05.030>
- [22] Reddy, JV Ramana, V. Sugunamma, N. Sandeep and C. Sulochana. "Influence of chemical reaction, radiation and rotation on MHD nanofluid flow past a permeable flat plate in porous medium." *Journal of the Nigerian Mathematical Society* 35, no. 1 (2016): 48-65. <https://doi.org/10.1016/j.jnnms.2015.08.004>
- [23] Bhatti, Muhammad Mubashir, S. R. Mishra, Tehseen Abbas and Mohammad Mehdi Rashidi. "A mathematical model of MHD nanofluid flow having gyrotactic microorganisms with thermal radiation and chemical reaction effects." *Neural Computing and Applications* 30 (2018): 1237-1249. <https://doi.org/10.1007/s00521-016-2768-8>
- [24] Tistomo, Arfan Sindhu and Aditya Achmadi. "Thermal radiation effect measurement in enclosure calibration." In *Journal of Physics: Conference Series*, vol. 2498, no. 1, p. 012022. IOP Publishing, 2023. <https://doi.org/10.1088/1742-6596/2498/1/012022>
- [25] Shah, Syed Amir Ghazi Ali, Ali Hassan, Hanen Karamti, Abdullah Alhushaybari, Sayed M. Eldin and Ahmed M. Galal. "Effect of thermal radiation on convective heat transfer in MHD boundary layer Carreau fluid with chemical reaction." *Scientific Reports* 13, no. 1 (2023): 4117. <https://doi.org/10.1038/s41598-023-31151-4>
- [26] Harish, Modalavalasa, Shaik Mohammed Ibrahim, Parthi Vijaya Kumar and Giulio Lorenzini. "A study on effects of thermal radiative dissipative MHD non-Newtonian nanofluid above an elongating sheet in porous medium." *Journal of Applied and Computational Mechanics* 9, no. 4 (2023): 945-954.
- [27] Magyari, E. and B. Keller. "Heat and mass transfer in the boundary layers on an exponentially stretching continuous surface." *Journal of Physics D: Applied Physics* 32, no. 5 (1999): 577. <https://doi.org/10.1088/0022-3727/32/5/012>
- [28] Bidin, Biliana and Roslinda Nazar. "Numerical solution of the boundary layer flow over an exponentially stretching sheet with thermal radiation." *European journal of scientific research* 33, no. 4 (2009): 710-717.
- [29] Ishak, Anuar. "MHD boundary layer flow due to an exponentially stretching sheet with radiation effect." *Sains Malaysiana* 40, no. 4 (2011): 391-395.
- [30] Khan, Umair, Aurang Zaib, Ioan Pop, Iskandar Waini and Anuar Ishak. "MHD flow of a nanofluid due to a nonlinear stretching/shrinking sheet with a convective boundary condition: Tiwari–Das nanofluid model." *International Journal of Numerical Methods for Heat & Fluid Flow* 32, no. 10 (2022): 3233-3258. <https://doi.org/10.1108/HFF-11-2021-0730>
- [31] Khan, Umar, Zafar Mahmood, Sayed M. Eldin, Basim M. Makhdom, Bandar M. Fadhl and Ahmed Alshehri. "Mathematical analysis of heat and mass transfer on unsteady stagnation point flow of Riga plate with binary chemical reaction and thermal radiation effects." *Heliyon* 9, no. 3 (2023). <https://doi.org/10.1016/j.heliyon.2023.e14472>
- [32] Vijaya, Kolli and Bommanna Lavanya. "Chemical Reaction Effects on of Nanofluid Past a Permeable Stretching Sheet with Slip Boundary Conditions and MHD Boundary Layer Flow." *International Journal of Heat & Technology* 40, no. 6 (2022). <https://doi.org/10.18280/ijht.400622>



- [33] Li, Shuguang, Kodi Raghunath, Ayman Alfaleh, Farhan Ali, A. Zaib, M. Ijaz Khan, Sayed M. Eldin and V. Puneeth. "Effects of activation energy and chemical reaction on unsteady MHD dissipative Darcy–Forchheimer squeezed flow of Casson fluid over horizontal channel." *Scientific reports* 13, no. 1 (2023): 2666. <https://doi.org/10.1038/s41598-023-29702-w>
- [34] Salah, Faisal and Abdelmgid OM Sidahmed. "Chemical Reaction and Radiation Effects on MHD Flow of Oldroyd-B Fluid through Porous Medium Past an Exponentially Stretching Sheet with Heat Sink." *Journal of Applied Mathematics* 2022, no. 1 (2022): 6582295. <https://doi.org/10.1155/2022/6582295>
- [35] Mahabaleshwar, U. S., T. Anusha, O. Anwar Bég, Dhananjay Yadav and Thongchai Botmart. "Impact of Navier’s slip and chemical reaction on the hydromagnetic hybrid nanofluid flow and mass transfer due to porous stretching sheet." *Scientific Reports* 12, no. 1 (2022): 10451. <https://doi.org/10.1038/s41598-022-14692-y>
- [36] Singh, Khilap and Manoj Kumar. "Influence of chemical reaction on heat and mass transfer flow of a micropolar fluid over a permeable channel with radiation and heat generation." *Journal of Thermodynamics* 2016, no. 1 (2016): 8307980. <https://doi.org/10.1155/2016/8307980>
- [37] Roja, Parakapali, Thummala Sankar Reddy, Shaik Mohammed Ibrahim, Meruva Parvathi, Gurram Dharmiah and Giulio Lorenzini. "Magnetic Field Influence on Thermophoretic Micropolar Fluid Flow over an Inclined Permeable Surface: A Numerical Study." *Journal of Applied and Computational Mechanics* 10, no. 2 (2024): 369-382.
- [38] Mukhopadhyay, Swati. "Slip effects on MHD boundary layer flow over an exponentially stretching sheet with suction/blowing and thermal radiation." *Ain Shams Engineering Journal* 4, no. 3 (2013): 485-491. <https://doi.org/10.1016/j.asej.2012.10.007>
- [39] Mabood, Fazle, W. A. Khan and Al Md Ismail. "MHD flow over exponential radiating stretching sheet using homotopy analysis method." *Journal of King Saud University-Engineering Sciences* 29, no. 1 (2017): 68-74. <https://doi.org/10.1016/j.jksues.2014.06.001>
- [40] Mandal, Iswar Chandra, Swati Mukhopadhyay and Kuppalapalle Vajravelu. "Melting heat transfer of MHD micropolar fluid flow past an exponentially stretching sheet with slip and thermal radiation." *International Journal of Applied and Computational Mathematics* 7 (2021): 1-18. <https://doi.org/10.1007/s40819-021-00955-1>
- [41] Lavanya, Bommanna and Madduleti Nagashashikala. "Effects of chemical reaction and heat generation on the unsteady free convection flow past an infinite vertical permeable moving plate with variable temperature." *Journal of Advanced Research in Fluid Mechanics and Thermal Sciences* 64, no. 2 (2019): 244-252.